STABILITY BEHAVIOR OF LIGHTWEIGHT AGGREGATE CONCRETE FILLED STEEL TUBULAR COLUMNS UNDER AXIAL COMPRESSION

Bohai Ji*, Zhongqiu Fu, Tao Qu and Manman Wang

College of Civil and Transportation Engineering, Hohai University, Nanjing 210098, China
**(Corresponding author: E-mail: hhbhji@163.com)*

Received: 10 August 2011; Revised: 26 October 2011; Accepted: 14 November 2011

ABSTRACT: Based on the previous study of the lightweight aggregate concrete filled steel tube (LACFST) slender columns, LACFST specimens with larger slenderness ratio from 64 to 96 were tested. According to the test results, the stability behavior was studied and its influence factors were analyzed. The bound slenderness ratio value was judged and the calculation method was studied. The test results demonstrated that LACFST slender columns under axial compression were damaged instability, and the value of bearing capacity and stability factor decrease as the slenderness ratio increases. Based on the test results analysis, the bound slenderness ratio of LACFST is 80 in this test. A method based on the Euler formula to calculate bound slenderness ratio is provided, and the calculation results are consistent with test ones. By comparison, it is found that the bound slenderness ratio of LACFST is smaller than that of normal CFST. The calculation results using Euler formula indicates that the bearing capacity can be calculated using Euler formula when the LACFST slender columns slenderness ratio is larger than the bound value.

Keywords: Lightweight aggregate concrete filled steel tube, Axial compression, Stable, Bound slenderness ratio, Euler formula

1. INTRODUCTION

Concrete filled steel tube (CFST) has the excellence of high bearing capacity, good seismic performance, small cross-sectional area and convenient construction. It has been widely studied and used in projects [1,2,3,4,5]. Lightweight aggregate concrete (LAC) can be produced from solid waste, and is about 20% to 30% lighter than normal concrete. Therefore, LAC is an environmental material which can be used in engineering to reduce the self weight [6,7,8]. If LAC is filled into steel tube, it forms lightweight aggregate concrete filled steel tube (LACFST). Similar to normal CFST, the buckling of steel pipe is delayed by LAC, and the LAC compressive strength is increased by the confinement of steel pipe. At the same time, the lower elastic modulus and higher brittleness of LAC are also improved. Because of the lightweight characteristic and good performance, LACFST has good application prospect. Especially in the long span bridge and high-rise building structures, the crossover ability will be increased and the foundation cost will be reduced.

Compared to normal CFST and LAC, the studies and applications about LACFST are less according to the literature number. In recent years, more and more scholars start to study the behavior of LACFST. The test by Assi and Qudeimat showed that LAC can enlarge the bearing capacity of steel pipe [9]. The study by Ghannam and Jawad indicated that LAC can replace normal concrete to fill in the steel tube in composite structural [10]. From the test result, Mouli found that LAC offered higher bond strength than normal concrete and contribution of LAC to the squash load were shown to be considerable [11]. Japan had used LACFST in "Shinkansen" project (high-speed railway bridge) [12]. In China, Li tested a lot of self stress lightweight concrete and gangue concrete filled steel tubular specimens [13, 14]. Ding and Yu analyzed the Nonlinear Properties of LACFST [15]. He tested 16 square thin-walled stub LACFST columns and proposed mechanical model [16]. Gao and Li studied the seismic behavior of LACFST frame in experimental way [17].

In spite of that, the study about the performance of LACFST is still in a primary stage. The author has studied the behavior of LACFST stub columns and slender columns whose slenderness ratio is from 12 to 56 [18, 19]. The influence of different parameters was surveyed, including steel and LAC strength, steel ratio, slenderness ratio, and so on. It was found that slenderness ratio impacts on the behavior more and more obvious as the LACFST column length increases. As a further study on the behavior of slender column, the stability of LACFST with the larger slenderness ratio from 64 to 96 was studied in this paper.

2. EXPERIMENTAL INVESTIGATIONS

2.1 Materials

The coarse aggregate of lightweight aggregate concrete is shale ceramic. The physical and mechanical properties are as following: lightweight aggregate bulk density is 814 kg/m^3, cylindrical compression strength is 8.5MPa, the ratio of water absorption ratio is 6% per hour. Ordinary Portland cement is used in this test. Materials are mixed by concrete mixer. According to the relevant Chinese standards, compression tests were carried out on a number of Standard cubes ([150×150×150] mm) to determine the concrete grade, and prisms ([150×150×300] mm) in order to determine the 28-days compressive strength (f_{ck}) and elastic modulus (E_c) of the unconfined concrete. The cubes and prisms were conditioned at room temperature. The concrete mixture is shown in Table 1 and the material properties are shown in Table 2.

Table 1. Mixture Mass for per Cubic Meter LAC Concrete

Cement (kg)	Haydite (kg)	Sand (kg)	Water (kg)
460	670	650	170

Table 2. Properties of LAC Concrete

Cubic strength f_{cu} (MPa)	Prism strength f_{ck} (MPa)	Elastic Modulus E_c (GPa)	Bulk density (kg/m^3)
44.7	35.2	26.2	1810

Straight welded steel tube Q235 was used in the test. A group of three standard specimens which were cut from each thickness of steel tube were tested to determine the tensile strength of the steel. Test method followed the regulations of Chinese standard "Metallic materials at ambient temperature tensile test method" (GB/T228, 2002). The data was collected by TS3890 pseudo-dynamic strain instrument in the whole process. Two kinds of steel tubes with thicknesses of 2.9mm and 3.5mm respectively were tested. Because the tested results are very close, Yield strength 274.7MPa was used for convenience. The stress and strain relationship of specimen is shown in Figure 1.

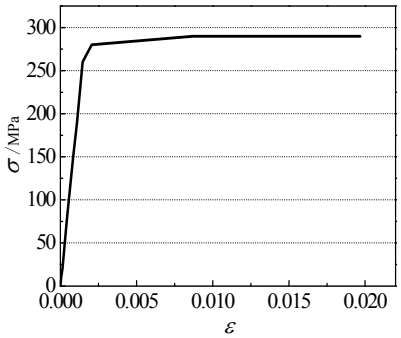

Figure 1. Stress Versus Strain Curve of Steel

2.2 Specimens

Steel tubes were processed according to the required length, and the two ends were polished flat. Each column was welded with a 10 mm thick circular endplate on one end before pouring concrete. The LAC was filled into steel tube with 500mm thickness for each layer. A 50mm diameter vibrating rod was used to vibrate concrete to ensure its density after pouring work finished. The specimens were maintained in natural conditions. After 10 days conservation, another end was smoothed with cement mortar, and welded with a 10mm thick circular endplate. The parameters of LACFST specimens are given in Tables 3 together with the results which will be discussed later.

Table 3. Detail of the Test Specimens

Specimens	Pipe size (mm)			λ	α（%）	N_u(kN)	$\overline{N_u}$（kN）	$\varphi=N_u/N_o$
	D	t	L					
A-3-a	114	2.9	342	12	11.00	814.76		1.002
A-3- b	114	2.9	342	12	11.00	850.87	813.02	1.046
A-3- c	114	2.9	342	12	11.00	773.44		0.951
A-16-a	114	2.9	1824	64	11.00	739.50		0.910
A-16-b	114	2.9	1824	64	11.00	780.56	743.95	0.960
A-16-c	114	2.9	1824	64	11.00	711.81		0.876
A-20-a	114	2.9	2280	80	11.00	648.00		0.797
A-20-b	114	2.9	2280	80	11.00	728.00	692.00	0.895
A-20-c	114	2.9	2280	80	11.00	700.00		0.861
A-24-a	114	2.9	2736	96	11.00	548.50		0.675
A-24-b	114	2.9	2736	96	11.00	448.00	501.17	0.551
A-24-c	114	2.9	2736	96	11.00	507.00		0.624
B-3-a	114	3.5	342	12	13.51	865.28		0.980
B-3-b	114	3.5	342	12	13.51	863.72	883.16	0.979
B-3-c	114	3.5	342	12	13.51	920.50		1.042
B-16-a	114	3.5	1824	64	13.51	773.00		0.875
B-16-b	114	3.5	1824	64	13.51	747.05	753.38	0.846
B-16-c	114	3.5	1824	64	13.51	740.10		0.838
B-20-a	114	3.5	2280	80	13.51	—		—
B-20-b	114	3.5	2280	80	13.51	701.01	703.00	0.794
B-20-c	114	3.5	2280	80	13.51	705.00		0.798
B-24-a	114	3.5	2736	96	13.51	615.03		0.696
B-24-b	114	3.5	2736	96	13.51	558.01	592.50	0.632
B-24-c	114	3.5	2736	96	13.51	604.46		0.684

Note: 1. D is the external diameter, t is the thickness, L is the length of specimen,
2. f_y is the yield strength of steel, λ is the slenderness ratio, $\lambda=4L/D$;
3. α is steel ratio, $\alpha=A_s/A_c$, here A_s is the area of steel, A_c is the area of concrete;
4. N_u is test ultimate load, $\overline{N_u}$ is the average value of test ultimate load for each group;
5. φ is stability factor, $\varphi=N_u/N_o$, here N_o is test ultimate load of short column(L/D=3).

2.3 Test Instruments and Procedure

Figure 2 shows the details of the test instruments. The experiment was performed in the structural engineering laboratory of Hohai University. Hydraulic jack was implemented to apply load on the specimen, and pressure sensor was used to measure load value. At the two ends of the specimen, column, support plate were utilized to simulate the hinged boundary condition.

In order to reduce the adverse effect of initial imperfection, several methods were adopted. They were as follows: ① Steel pipe surface were examined carefully; ② two ends of the steel pipe were polished flat; ③ the end was smoothed with cement mortar before the second endplate wedded; ④ a bolt was inserted in the holes which were set on the center of the endplate and support plate (Figure 2); ⑤ a plumb line was used as reference at the side of the specimen when loading (Figure 2). In these ways, it can ensure the specimen was vertical and the load was added axially as much as possible.

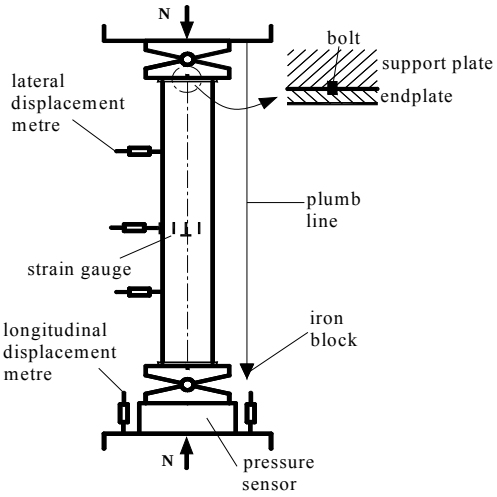

Figure 2. Loading and Measurement System

(a)A-16 (b) B-20 (c) A-24

Figure 3. Failure specimens

For the accuracy of the specimen's deformation measurement, strain gauges were set at the mid-length of the column to record longitudinal strain and transverse strain. On the reaction frame, three lateral displacement meters were set to measure the deflection at quadrant point along the length of the column. And two longitudinal displacement meters were set to measure the longitudinal deformation. All data was recorded by computer data acquisition system in the whole test phase. The specimen was loaded at rate of 1/10 of the predicted ultimate load in the elastic phase and at loading rate of 1/15 of the predicted ultimate load in the column yielding phase. Each load was maintained for 2-3 minutes to enable the full deformation development. When approaching the predicted ultimate capacity, the load was added slowly.

3. DISCUSSIONS OF TEST RESULTS

3.1 Test Phenomenon

Figure 3 shows some typical failure specimens. No local buckling phenomenon was observed. All slender columns specimens failed because of excessive lateral deformation, and damaged instability under axial compression. When jack was loaded off after the experiment, majority bending deformation of slender columns could be resumed, which meant the majority of the deflection was elastic deformation when the specimen was damaged under loading.

Deflection distribution along the length under different load is shown in figure 4. For most specimens, as the load increased, deflection increased gradually with the largest value at middle point and symmetrical growth at two sides (Figure 4a). The curves shape is similar with the sine half-wave. However, due to initial defects containing material discontinuity and load eccentricity and so on, the deflection developed asymmetry for some specimens as shown in Figure 4(b). However, the deflection was rectified as the load increasing. The deflection distribution tended to

symmetry. The largest deflection value appeared at the middle point when the specimen was destroyed finally.

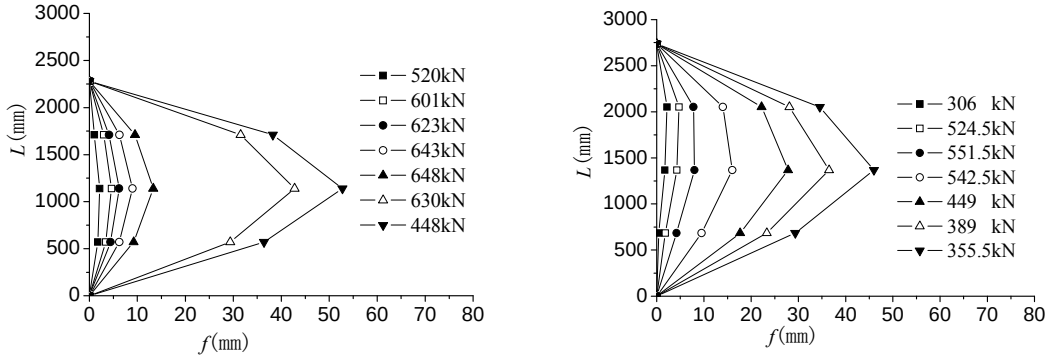

(a) A-20-a (b) B-24-b

Figure 4. Deflection Distribution Along the Length as the Load Increasing

3.2 Failure Process

Figure 5 is load N – midpoint deflection f curves. Because of initial defects, the deflection of some specimens developed at the beginning of test. At the loading initial stage, the deflection increased slowly. When the load was about 60% to 70% of ultimate load, lateral deflection and vertical displacement increased rapidly. When reaching the ultimate load, deflection increased more quickly, and the load became coming down. The larger slenderness ratio led to the more quickly deflection increased. This is because larger slenderness ratio has smaller bending stiffness, and will produce larger additional bending moment.

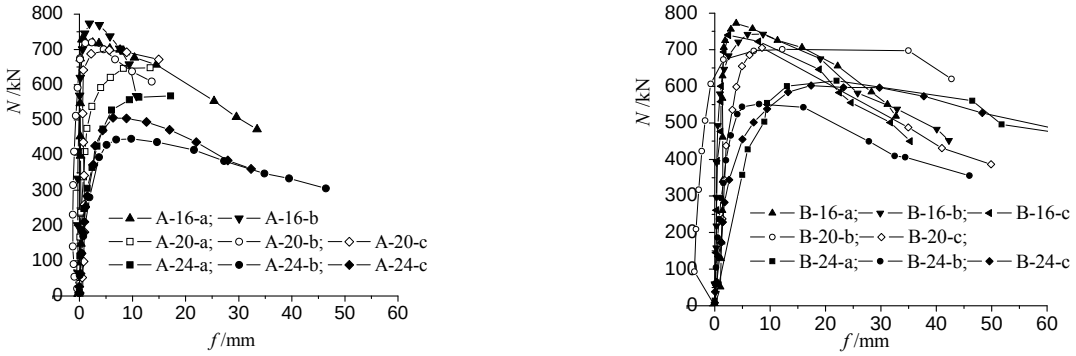

(a) (b)

Figure 5. Load (N) – Midpoint Displacement (f) Curves

3.3 Strain analysis

Figure 6 is the load (N)- strain (ε)curves at middle partial. It reflects the development of longitudinal and hoop stain of the steel which were obtained by strain gauge set on the steel pipe. Point a and b represent the specimen on two sides divided by roll shaft. Point a is the middle side of flexural specimen, and point b is the lateral side of flexural specimen.

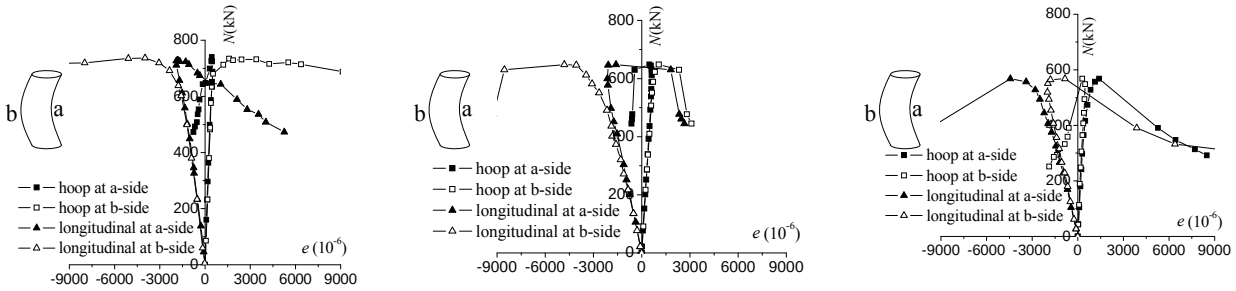

(b)A-16-a (c)A-20-a (d)A-24-a

Figure 6. Load (N)- Strain (ε) Curves at Middle Partial

From the figures, it can be seen that, at the beginning of load application, the whole cross-section of specimen was under pressure. The differences of longitudinal strain at two sides were not obvious. Achieved about 70% of the ultimate load, longitudinal strain at a-side became growing slower than b-side. After reaching the ultimate load, longitudinal strain in a-side reduced and became to be tensile strain finally. At the same time, the opposite situation occurred for hoop strain at a-side. This is because the deflection produced additional bending moment, and this made the specimen under the situation that one side was bearing tension and another side was bearing compression.

The lateral deformation coefficient μ is defined similar as Poisson's ratio in order to reflect whether the material has yielded or not. In general, Poisson's ratio of steel is 0.25~0.3. If the lateral deformation coefficient is less than 0.3, the steel is in elastic stage. The lateral deformation coefficient can be calculated by equation (1). In the equation, ε_{sh} is the hoop strain and ε_{sl} is the longitudinal strain of the steel at middle point. They were measured by the strain gauges on the steel tube.

$$\mu = \varepsilon_{sh} / \varepsilon_{sl} \tag{1}$$

Figure 7 is the lateral deformation coefficient variation curves of specimen. Positive and negative values are used to distinguish the two side. One group of same section specimens is selected to prove that the curves of specimens with same parameter are similar. Therefore, one of them can represent a group. Based on this, one of each group specimens with different slenderness ratio is selected to compare with each other.

It can be found that the lateral deformation coefficient of specimen is close to Poisson's ratio of steel in the initial loading state. It indicates that the steel are at the elastic stage, and there is no obvious constraining stress between concrete and steel. At the beginning, variation trend of stub column and slender column is the same. When it reached to 70% of ultimate load for stub column (L/D=3), the lateral deformation coefficient became increscent and exceeded Poisson's ratio of steel. This produced constraining stress between concrete and steel. It made the strength of materials used fully. While for the slender column, the lateral deformation coefficient became increscent when it reached to the ultimate load. At this moment, the specimen had already been damaged. This indicates that strength of the material is not fully used when the slender column is damaged.

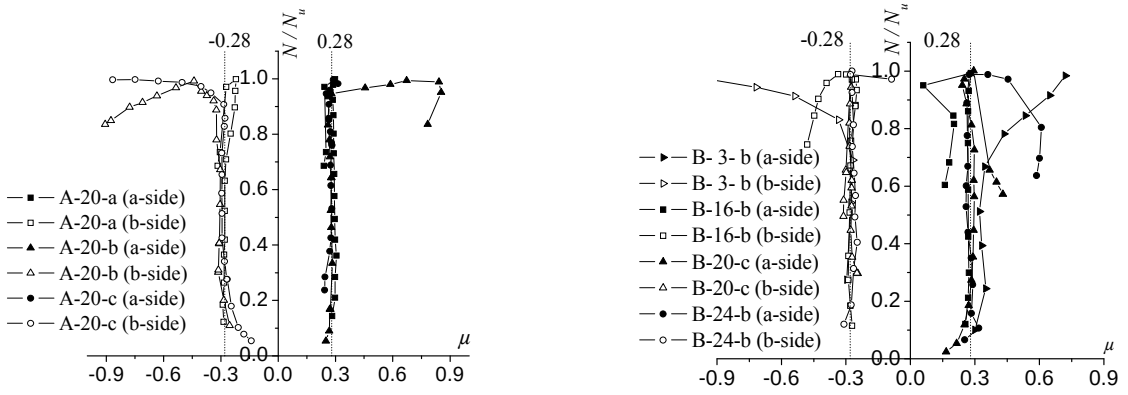

(a) One group specimens (b) Different slenderness ratio specimens

Figure 7. Lateral Deformation Coefficient Variation Curves of Specimens

3.4 Influence of Slenderness Ratio

The behavior of LACFST slender column had been studied by 11 group specimen tests in author's previous study [19]. And group SC2 in previous test has the same section parameter with group B in this test. The stub column bearing capacity of group SC2-3 is 887.5kN and group B-3 is 883.2kN. They are very close to each other. Therefore, these two groups can be compared together.

Figure 8 shows the deflection development as load increasing with the *L/D* from 7 to 24. From the figure, deflection of specimen with larger slenderness ratio increased more quickly as the loading increases. After ultimate load, the specimen curve which has larger slenderness ratio develops more gently. This is because the initial defects impact more obviously when the specimen has a larger slenderness ratio.

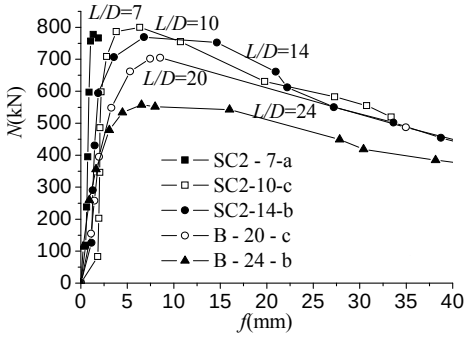

Figure 8. *N-f* curves of Different *L/D*

Figures 9 and 10 show the development of bearing capacity (N_u) and stability factor (φ) as the *L/D* increases. The average value is used in the figures. It indicates that the bearing capacity and stability factor decrease as the slenderness ratio increases. This is the same conclusion with the result studied before which *L/D* is from 3 to 14.

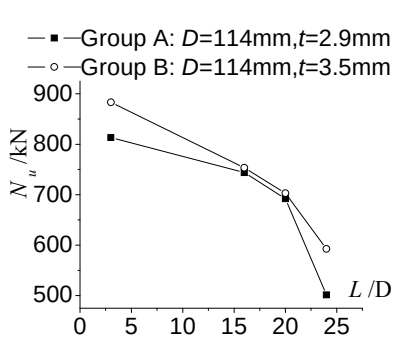

Figure 9. N_u-L/D Curves

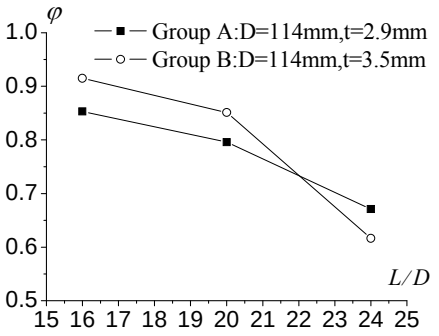

Figure 10. φ-L/D Curves

4. BOUND SLENDERNESS RATIO ANALYSIS

4.1 Bound Slenderness Ratio Judgment

The longitudinal strain ε_c of specimen can be obtained from expression (2). In the expression, Δ is the longitudinal compression displacement measured by displacement meters, L is the length of the specimen.

$$\varepsilon_c = \Delta / L \tag{2}$$

As stated above, group SC2 studied before and group B studied in this test can be compared together. Figure 11 shows the longitudinal strain development with the load increases. From the figure, the specimen with smaller slenderness ratio has larger bearing capacity and longitudinal strain. The smaller the slenderness ratio, the more significant plastic deformation and the material strength played more fully. When $\lambda \geq 80$ (group B-20 and B-24 specimens), curves change from upward trend to downward trend directly without transition process. The specimen is in the elastic state when it reaches ultimate load.

Lateral deformation coefficient μ corresponding with ultimate load is analyzed to study whether the material has yielded or not. The lateral deformation coefficient was defined in equation (1) above. Its development as the slenderness ratio increases is shown in Figure 12.

The larger the slenderness ratio is, the smaller the lateral deformation coefficient is. When it reaches ultimate load, specimen bend to lateral side (b-side). It causes the longitudinal strain to change from compression to tension. Therefore, μ corresponding with ultimate load is larger at medial side (a-side) than that at lateral side (b-side). Compared to Poisson's ratio of steel, considering experimental error, it can be deemed that steel is in the elastic stage when $\mu \leq 0.3$. From figure 12, with slenderness ratio $\lambda \geq 80$, lateral deformation coefficient $\mu \leq 0.3$ when it is ultimate load. Therefore, from the test results it can be concluded that specimen is elastic failure when it reaches to ultimate load with $\lambda \geq 80$ in the parameter range of this test.

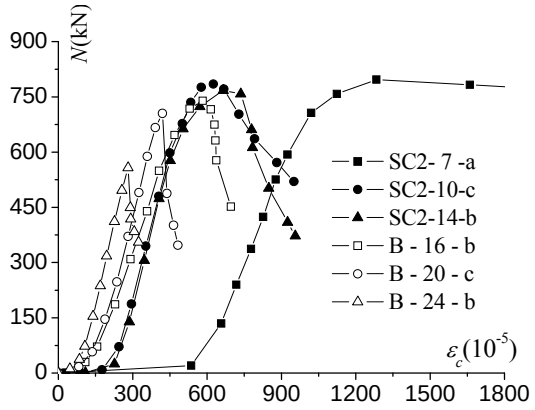

Figure 11. N- ε_c Curves

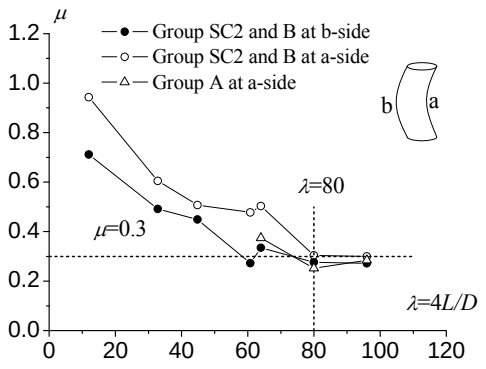

Figure 12. μ - λ Curves when Ultimate Load

4.2 Bound Slenderness Ratio Calculation

For the slender column, if its slenderness ratio is large enough, the column is damaged abruptly because of excessive deflection with the material also in elastic stage. This is elastic failure. If the material is in elastic-plastic stage when column damaged, it is elastic-plastic failure. The bound slenderness ratio λ_p is the boundary between the two failure modes. When slenderness ratio of columns is less than λ_p, it will be elastic-plastic failure. Otherwise, it will be elastic failure. According to stability theory, Euler formula can be used to calculate the bearing capacity of slender column when it is elastic failure. And the critical stress σ_{cr} can be got from equation (3). E_{sc} is the elastic modulus of LACFST specimen.

$$\sigma_{cr} = \pi^2 E_{sc} / \lambda^2 \tag{3}$$

If the column is elastic failure, its limit of proportionality f_{sc}^p will larger than or equal to critical stress $\sigma_{cr.}$ In order to know the bound slenderness ratio λ_p , the value of σ_{cr} can be taken as f_{sc}^p. Equation (4) can be used to calculate λ_p. Based on the study of LACFST stub column, f_{sc}^p takes the sectional stress which corresponds to 85% bearing capacity of stub column [18].

$$\lambda_p = \sqrt{\pi^2 E_{sc} / f_{sc}^p} \tag{4}$$

According to the study of LACFST stub column, the LACFST elastic modulus E_{sc} can be got as equation (5). $E_{sc,}$ $E_{s,}$ E_c is elastic modulus of LACFST, steel, LAC; $A_{sc,}$ $A_{s,}$ A_c is sectional area of LACFST, steel, LAC.

$$E_{sc} A_{sc} = E_s A_s + E_c A_c \tag{5}$$

Equation (4) is used to calculate the bound slenderness ratio of specimens in this test. The results are listed in Table 4.

Table 4. Calculation Results of Bound Slendemess Ratio

Specimen group	E_{sc} (MPa)	N_u (kN)	f_{sc}^p (MPa)	Calculation results of λ_p		
				Equation (4)	Equation (6)	Equation (7)
SC1	30.63×10^3	927.30	36.88	90.49	101	95.2
SC2	50.60×10^3	887.60	73.95	82.13	98	89.2
SC3	41.70×10^3	742.54	61.87	81.52	98	93.6
A	44.21×10^3	813.02	67.74	80.22	105	96.4
B	47.78×10^3	883.16	73.58	80.01	105	96.8

Two formulas of normal CFST are also used to calculate λ_p, the results of which are also listed in Table 4. The calculation formulas are described with following equations. Equation (6) is a simple empirical formula [20]. Equation (7) is deduced through modifying the formulas by tangent modulus method [15].

$$\lambda_p = 1743/\sqrt{f_s} \tag{6}$$

$$\lambda_p = \pi\eta\sqrt{\gamma E_s/(\theta f_s)} \tag{7}$$

Coefficient η, γ, θ can be got by equations (8) to (10). In the equations, f_s and f_c is the strength of steel and concrete.

$$\eta = \frac{0.73 f_s/f_c - 1.7}{f_s/f_c - 31} \le 1 \tag{8}$$

$$\gamma = \frac{2n\rho + 1 - 2\rho}{n\rho + 1 - \rho} > 1 \tag{9}$$

$$\theta = f(\rho) + \frac{1 - f(\rho)}{5.5\times10^{-3}(f_s/f_c)^{2.6} + 1} \tag{10}$$

$$f(\rho) = 0.48 + 3.19\rho^{1.62},\ \rho = A_s/A_{sc},\ n = E_s/E_c \tag{11}$$

From Table 4, the bound slenderness ratio of specimen in this test is about 80. It is the same conclusion as the judgment from the strain analysis of test results. Therefore, the following conclusion can be got that bound slenderness ratio of specimens is 80 in this test. And the method provided in this paper is reasonable for calculating bound slenderness ratio of LACFST. With the comparison among three equations, the results of equation (4) are smaller than the other two. It indicates that the bound slenderness ratio of LACFST is less than the one of normal CFST. The calculation method for normal CFST can not be used directly to LACFST.

4.3 Failure Mode Judgment

According to stability theory, the bearing capacity of slender columns can be calculated using Euler formula. The value of Elastic modulus takes into Euler formula, the ultimate bearing capacity P_{cr} can be got. Figure 13 is the comparison between Euler formula and test result. When the specimens are elastic failure ($\lambda\ge80$), test result has the same development trend with Euler formula calculation line. The largest deviation between the two is less than 15%. Therefore, it can be taken that the Euler formula result is tally with the test result well.

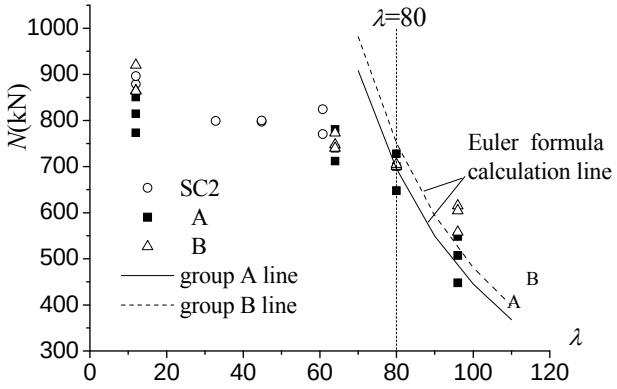

Figure 13. Comparison between Euler Formula and Test

The test and Euler formula calculation values of bearing capacity are listed in Table 5. Because Euler formula applies for the columns with $\lambda \geq \lambda_p$, the calculation value using Euler formula will obviously larger than the actual value when $\lambda \leq \lambda_p$. As the same mean, it is elastic-plastic failure when the calculation value using Euler formula is obviously larger than the actual value. Otherwise, it is elastic failure. From Table 5, it has an obvious deviationt between the two bearing capacity of specimen with λ=64. While the two bearing capacity values of specimen with λ=80 and λ=96 are close to each other. This indicates that it is elastic-plastic failure when λ=64, and it is elastic failure λ=80 and λ=96. This proves that the bound slenderness ratio of LACFST specimen in this test is 80 which was obtained above.

Table 5. Test and Calculated Bearing Capacity Results Comparison

Specimen	Group name	A-16	A-20	A-24	B-16	B-20	B-24
	$\lambda=4L/D$	64	80	96	64	80	96
Calculation P_{cr}(kN)		1075.93	688.59	478.19	1161.15	743.14	516.07
Test P(kN)		743.95	692.00	501.17	753.38	703.00	592.50
P_{cr}/P		1.4462	0.9951	0.9541	1.5413	1.0571	0.8710

5. CONCLUSIONS

With larger slenderness ratio, the LACFST column under axial compression is easer to be failed by instability. And the bearing capacity and stability factor decrease as the slenderness ratio increases

Based on the test result analysis, the bound slenderness ratio of LACFST is 80 in the parameter range of this test. When the slenderness ratio is larger than 80, the failure mode of specimen is elastic failure. Otherwise, it is elastic-plastic failure.

According to stability theory, a method based on the Euler formula to calculate bound slenderness ratio is provided，and the calculated outcome is consistent well with test result. The bound slenderness ratio of LACFST is smaller than the value calculated using experimental formula of normal CFST.

For the LACFST column with larger slenderness ratio than the bound one, the bearing capacity can be calculated using Euler formula approximately.

ACKNOWLEDGMENTS

The authors appreciate the support of China Postdoctoral Science Foundation (2012M511187), The Fundamental Research Funds for the Central Universities (2012B02914), and Jiangsu Civil Engineering Graduate Center for Innovation and Academic Communication foundation (2010).

REFERENCES

[1] Ge, H.B., Susantha, K.A.S., Satake, Y., et al., "Seismic Demand Predictions of Concrete-filled Steel Box Columns", Engineering Structures, 2003, Vol. 25, No. 3, pp. 337-345.

[2] Gao, S.B. and Ge, H.B., "Numerical Simulation of Hollow and Concrete-filled Steel Columns", Int. J. of Advanced Steel Construction, 2007,Vol. 3, No. 3, pp. 668-678.

[3] Yang, Y.F., Han L.H. and Zhu L.T., "Experimental Performance of Recycled Aggregate Concrete-Filled Circular Steel Tubular Columns Subjected to Cyclic Flexural Loadings", Advances in Structural Engineering, 2009, Vol. 12, No. 2, pp. 183-194.

[4] Dabaon, M.A., El-Boghdadi, M.H. and Hassanein, M.F., "Experimental Investigation on Concrete-filled Stainless Steel Stiffened Tubular Stub Columns", Engineering Structures, 2009, Vol. 31, No. 2, pp. 300-307.

[5] Nakamura, S. Tanaka, H, and Kato, K., "Static Analysis of Cable-stayed Bridge with CFT Arch Ribs", Journal of Constructional Steel Research, 2009, Vol. 65, No. 4, pp. 776-783.

[6] Alengaram, U.J., Mahmud, H. and Jumaat, M.Z., "Comparison of Mechanical and Bond Properties of Oil Palm Kernel Shell Concrete with Normal Weight Concrete", International Journal of The Physical Sciences, 2010, Vol. 5, No. 8, pp. 1231-1239.

[7] Haque, M.N., Al-Khaiat, H. and Kayali, O., "Strength and Durability of Lightweight Concrete", Cement and Concrete Composites, 2004, Vol. 26, No. 4, pp. 307-314.

[8] Schaumann, E., Vallee, T. and Keller, T., "Modeling of Direct Load Transmission in Lightweight-Concrete-Core Sandwich Beams", ACI Structural Journal, 2009, Vol. 106, No. 4, pp. 435-444.

[9] Assi, I.M., Qudeimat, E.M. and Hunaiti, Y., "Ultimate Moment Capacity of Foamed and Lightweight Aggregate Concrete-filled Steel Tubes", Steel and Composite Structures, 2003, Vol. 3, No. 3, pp. 199-212.

[10] Ghannam, S., Jawad, Y.A. and Hunaiti, Y., "Failure of Lightweight Aggregate Concrete-filled Steel Tubular Columns", Steel and Composite Structures, 2004, Vol. 4, No. 1, pp. 1-8.

[11] Mouli, M. and Khelafi, H., "Strength of Short Composite Rectangular Hollow Section Columns Filled with Lightweight Aggregate Concrete", Engineering Structures, 2007, Vol. 29, No. 8, pp. 1791-1797.

[12] Nakamura, S., Momiyama, Y., Hosaka, T., et al., "New Technologies of Steel/Concrete Composite Bridges", Journal of Constructional Steel Research, 2002, Vol. 58, No. 1, pp. 99-130.

[13] Li, G.C., Liu, Z.Y., Feng, G.H., et al., "Bearing Capacity Calculation of Self Stress Lightweight Concrete Filled Steel Tubular Short Columns under Axial Compressive Loading", Journal of Northeastern University (Natural Science), 1997, Vol. 18, No. 6, pp. 636-639. (in Chinese)

[14] Li, G.C., Long, H.B., and Wang Z.Q., "Inelastic Yield Load of Gangue Concrete Filled Steel Tubular Middle Long Columns under Axial Compression", Journal of Shenyang Architecture and Civil Engineering University, 2004, Vol.20, No.4, pp. 291-293. (in Chinese)

[15] Ding F.X., Yu Z.W. and Jiang, L.Z. “Bearing Capacity of Middle Long Concrete filled Circular Steel Tubular Columns under Axial Compression”, China Journal of Highway and Transport, 2007, Vol. 20, No. 4, pp. 65-70. (in Chinese)

[16] He, M.S., and Liu, X.Y., “Study on Behavior of Lightweight Aggregate Concrete Filled Square Thin-walled Steel Tubes under Axial Load”, Journal of Harbin Institute of Technology, 2007, Vol. 39, No. supplement 2, pp. 78-81. (in Chinese)

[17] Gao, C.Y. and Li, B., “Experimental Research on Seismic Behavior for Lightweight Aggregate Concrete-filled Steel Tubular Frame”, Advanced Materials Research(Volumes 163-167), 2011, Vol. Advances in Structures, pp. 2194-2198.

[18] Fu, Z.Q., Ji, B.H., Zhou Y. and Wang X.L. “An Experimental Behavior of Lightweight Aggregate Concrete Filled Steel Tubular Stub under Axial Compression”, ASCE Geotechnical Special Publication, 2011, Vol. 219, pp. 24-32.

[19] Fu, Z.Q., Ji, B.H., Lv, L. and Zhou, W.J. “The Behavior of Lightweight Aggregate Concrete Filled Steel Tube Slender Columns under Axial Compression”, Advanced Steel Construction, 2011,Vol. 7, No. 2, pp. 144-156.

[20] Han, L.H. “Concrete Filled Steel Tube Structure: Theory and Practice”, Science Press, 2004 (in Chinese).